Available online at www.sciencedirect.com
SCIENCE DIRECT
Neurocomputing 69 (2006) 1053–1057
NEUROCOMPUTING
www.elsevier.com/locate/neucom

The role of action potential shape and parameter constraints in optimization of compartment models

Christina M. Weaver[a,b,c,*], Susan L. Wearne[a,b,c]

[a]Center for Biomathematical Sciences, Mount Sinai School of Medicine, New York, NY 10029, USA
[b]Computational Neurobiology and Imaging Center, Mount Sinai School of Medicine, New York, NY 10029, USA
[c]Department of Neuroscience, Mount Sinai School of Medicine, New York, NY 10029, USA

Available online 8 February 2006

Abstract

Automated parameter search methods are commonly used to optimize compartment model parameters. An important step in parameter fitting is selecting an objective function that represents key differences between model and experimental data. We construct an objective function that includes both time-aligned action potential shape error and errors in firing rate and firing regularity. We then implement a variant of simulated annealing that introduces a recentering algorithm to handle infeasible points outside the boundary constraints. We show how our objective function captures essential features of neuronal firing patterns, and why our boundary management technique is superior to previous approaches.

Keywords: Parameter search; Action potential; Optimization; Simulated annealing; Error

1. Introduction

Compartmental neuron models often have many parameters, only loosely constrained within physiologically plausible ranges, which are difficult to estimate manually. Parameter estimation can be facilitated by automated search methods that minimize an objective, or error function representing salient differences between simulated and experimental (''target'') data. Our interest lies in modeling neurons of the central vestibular system, for which firing regularity and dynamics vary widely across the population [15]. Action potential (AP) shape, including the shape of the afterhyperpolarization, has been shown to be a critical determinant of neuronal firing dynamics and discharge regularity [1,7]. Although previous modeling studies have included several important AP features and neuronal firing characteristics in their objective functions [16,18], few have included the entire AP shape. A recent study [4] calculated AP shape error as the mean-squared difference between target and model voltage traces, which yields large errors when the model and target APs differ even slightly in time. We present an objective function that avoids this problem by first aligning target and model APs, then calculating the root mean-squared (RMS) error. Our function also includes errors in firing rate and discharge regularity.

Vanier and Bower [18] recently found that simplex-based simulated annealing [10,13] can successfully optimize compartmental neuron models. We find that the performance of simulated annealing algorithm of Vanier and Bower [18] is impaired by the ''wraparound'' boundary condition they applied when the algorithm encounters an infeasible point in parameter space: one that lies outside the specified boundaries. Such a point lying beyond one side of the parameter space is relocated to the opposite side of the parameter space, by the amount of the overshoot. Our parameter search method uses a variant of simplex-based simulated annealing that avoids infeasible points by ''recentering'' such points about the current minimum [2].

*Corresponding author. Center for Mathematical and Computational Biology, Mount Sinai School of Medicine, New York, NY 10029, USA.
E-mail addresses: christina.weaver@mssm.edu (C.M. Weaver), susan.wearne@mssm.edu (S.L. Wearne).

0925-2312/$ - see front matter © 2006 Elsevier B.V. All rights reserved.
doi:10.1016/j.neucom.2005.12.044

We demonstrate that the recentering method is superior to the wraparound method, and that our objective function is effective in guiding the parameter search.

2. Methods

2.1. Mathematical model

The NEURON simulation environment [8] was used for this study. The efficacy of our optimization scheme and objective function (available online [11]) was tested using the six-conductance, single-compartment model of Av-Ron and Vidal [1] which can simulate the AP shapes and response dynamics of medial vestibular nucleus (MVN) neurons. The transient sodium (Na) and delayed rectifier potassium (K) currents were described by the Fitzhugh–Nagumo model [5,12]. Remaining active currents (transient A-type potassium (K(A)), high-voltage activated calcium (Ca), calcium-dependent potassium (K(Ca)), persistent sodium (NaP)), were described by Hodgkin–Huxley formalism. With these currents, membrane capacitance C_m ($\mu F/cm^2$), and passive leak conductance (L), membrane potential V was given by

$$C_m \frac{dV}{dt} = -I_{Na} - I_K - I_{K(A)} - I_{Ca} - I_{K(Ca)} - I_{NaP} - I_L, \quad (1)$$

where the current I_s for the ion species s was described by

$$I_s = \bar{g}_s a_s^{p_s} b_s^{q_s} (V - V_s). \quad (2)$$

Here, $\bar{g}_s$ is the maximal conductance of a membrane patch (mS/cm^2), a_s and b_s are the activation and inactivation variables with gating exponents p_s and q_s, respectively, and V_s is the reversal potential (mV). Equations describing the change in activation variables and ion channel kinetic parameters were taken directly from the MVN-model [1]. Changes in calcium concentration, C (mM), were described by

$$\frac{dC}{dt} = K_p(-I_{Ca}) - RC, \quad (3)$$

where K_p ($M\,cm^2/mC$) is an influx parameter converting calcium current to concentration, and R (1/ms) represents the calcium removal rate due to diffusion, buffering, and intracellular stores. Target data (Fig. 1A, dashed line) were generated by varying the parameters controlling maximal conductances and calcium kinetics to produce a model neuron which fires spontaneously at a frequency consistent with extracellular recordings of goldfish Area II neurons in vivo [15]. (see Table 1).

2.2. Objective function

Target and sample model data are shown in Fig. 1A. The objective function is a linear combination of AP shape, firing rate, and firing regularity error, with weights of 5, 10, and 100, respectively. AP shape error is determined by comparing the shape of the ith target AP within a time window W, centered on the AP peak, to the shape of the ith model AP within a similar window (Fig. 1B). Data in the target window are translated in time to align with data in the model window, and the root mean squared (RMS) error between the two traces is calculated separately for each model AP (Fig. 1C) over a 500 ms interval. The user specifies W before the search; APs are identified automatically. Instantaneous firing rates and discharge coefficient of variation (CV [17]) of the target and model data are also calculated. Differences between mean and standard deviation of these values comprise the firing rate and firing regularity errors.

Table 1
Parameters used to generate target data

Ion channel	$\bar{g}$ (mS/cm^2)	Passive parameters	
Na	10	$\bar{g}_L$ (mS/cm^2)	0.3
K	4	C_m ($\mu F/cm^2$)	1
K(A)	0	radius (μm)	15.5
Ca	0.25	Calcium parameters	
K(Ca)	1	K_p ($M\,cm^2/mC$)	0.05
NaP	0.05	R (1/ms)	0.0125

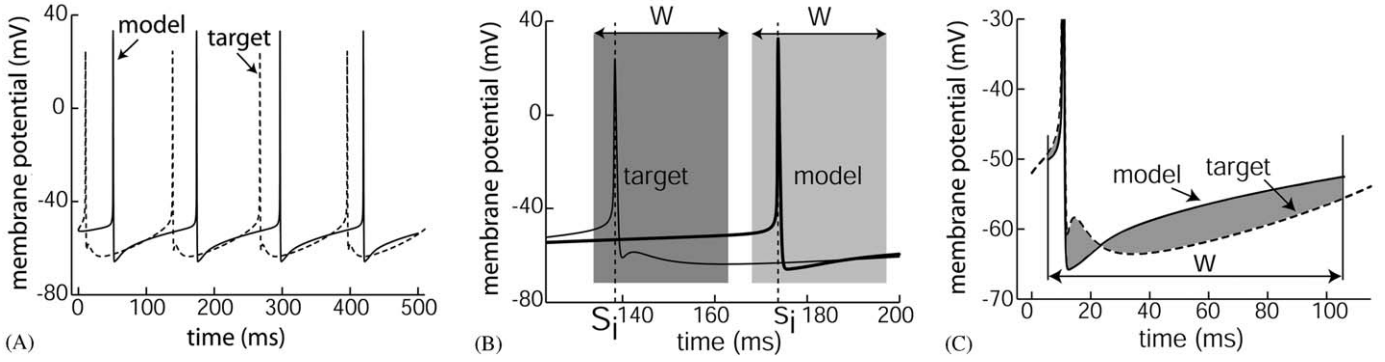

Fig. 1. (A) Target (dashed) and model (solid) data. (B) The window W, centered on the ith target AP (dark gray), and on the ith model AP (light gray). (C) Data contained in the model window are shifted to align with data in the target window. The RMS error between these traces comprises the AP shape error.

2.3. Simulated annealing

The recentering method [2] was implemented as a modification of the unconstrained simulated annealing algorithm [3,13]. The search visits consecutive points in parameter space [10,13]. Uphill moves are accepted with a probability proportional to a parameter that starts out high and decreases as the search continues. Each infeasible point is replaced by a point randomly selected from a temperature-dependent neighborhood of the current minimum [2].

2.4. Model optimization

Optimizations by the recentering and wraparound methods included either two parameters ($\bar{g}_{Na}$, $\bar{g}_K$) or seven parameters ($\bar{g}_{Na}$, $\bar{g}_K$, $\bar{g}_{K(A)}$, $\bar{g}_{K(Ca)}$, $\bar{g}_{Ca}$, K_p, R). Two-parameter searches were performed within narrow, biophysically plausible parameter ranges (N2), intermediate ranges (I2) and wide ranges (W2). Seven-parameter searches were performed for the narrow (N7) and intermediate (I7) parameter ranges. Robustness was evaluated by performing multiple searches from initial points chosen randomly within the narrow range ($n = 50$ searches for N2, N7, I2 and I7; $n = 20$ for W2).

2.5. Statistical methods

Each search returns a set of parameters corresponding to the optimal model encountered during the search and the associated model error, as determined by evaluation of the objective function. For each optimization condition (N2, N7, I2, I7, W2), we compared the error sets returned by wraparound and recentering methods, using the paired-samples t-test (normally distributed samples: Kolmogorov–Smirnov test) or the Wilcoxon signed rank test (non-normally distributed samples). The optimal parameters returned by each method were then compared to target values using either the one-sample t-test or the Wilcoxon signed rank test. A Bonferroni correction ensured an overall significance level of 0.05.

3. Results

Fig. 2A shows the median model error and 95% confidence interval of the N2 searches for the recentering (solid) and wraparound (dashed) methods, as a function of simulation number. Under this condition, the wraparound and recentering methods performed equally well. Under all other optimization conditions, the recentering method identified models with significantly smaller errors than the wraparound method, and identified them more quickly (Fig. 2B–D; W2 not shown). Whereas the voltage trace of the optimal recentering model (Fig. 2E, shifted vertically by 10 mV) from an N7 search superimposed with the target data, the optimal wraparound model exhibited a significant shape error (Fig. 2F).

The larger error of the wraparound method is a direct result of the imposed boundary condition. Fig. 3 shows ($\bar{g}_{Na}$, $\bar{g}_K$) pairs tested by the recentering (A) and wraparound (B) methods, for a two-parameter search with wide bounds. Dashed lines denote target values. The recentering method identified the target as its optimal model relatively

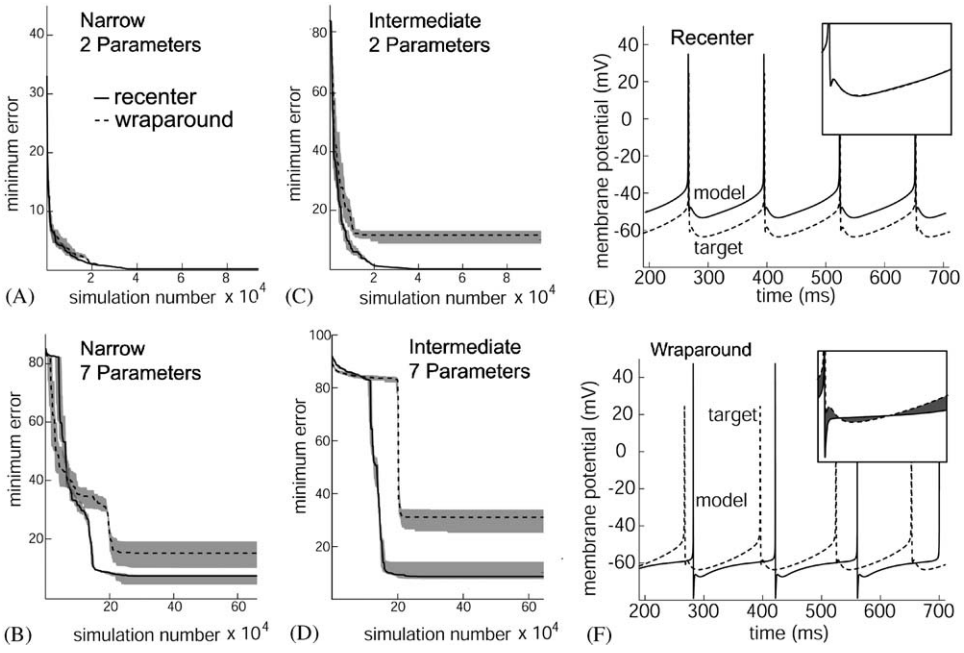

Fig. 2. (A–D) Minimum error vs. simulation number (median and 95% confidence interval) for the recenter (solid) and wraparound (dashed) boundary methods, for the (A) N2, (B) N7, (C) I2, and (D) I7 parameter searches. (E, F) Voltage traces for the optimal models (solid lines) identified from an N7 search for the (E) recenter and (F) wraparound condition, compared to target data (dashed). Insets show shape error detail. In (E), the model trace has been shifted vertically by 10 mV, otherwise traces would superimpose.

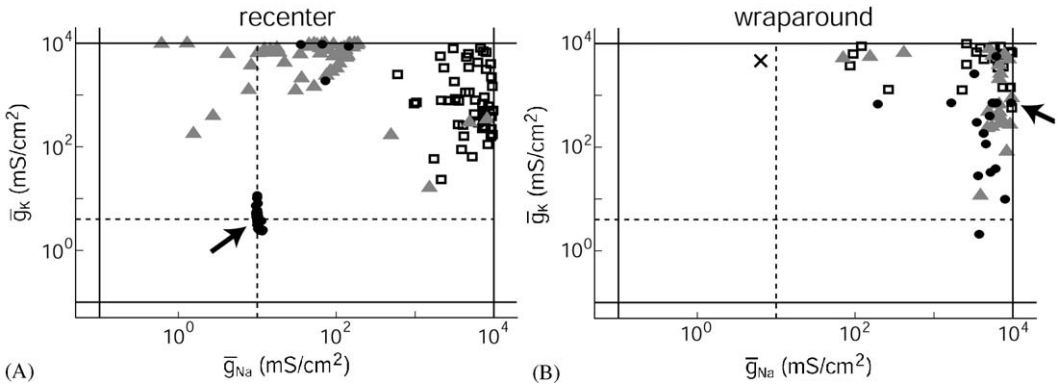

Fig. 3. Points tested for the recenter (A) and wraparound (B) methods for a W2 search. Points denote $(\bar{g}_{Na}, \bar{g}_K)$ pairs tested at early (open squares), intermediate (gray triangles), and late (black circles) times. Solid lines denote boundary constraints; dashed lines mark target values. Arrows show the point of search convergence. In (B), this point differs from the global minimum visited by the search, marked by an 'X'.

early in the search (black circles), and converged there (black arrow). In contrast, points visited by the wraparound method lie near the boundary (solid lines, Fig. 3B) almost exclusively. At a time in the search with a low probability of escaping a local minimum, the search algorithm encountered a value of $\bar{g}_{Na}$ below the lower boundary. The wraparound condition reassigned this point to one with a high $\bar{g}_{Na}$ value near the upper boundary. The search never recovered, converging to a point near the upper boundary (black arrow).

While the recentering method was superior in all optimization conditions, the efficiency of target parameter recovery varied with the difficulty of the problem. For two-parameter searches, both parameters were recovered reliably by the recentering method, however differences between target and optimal model parameters increased steadily with the number of parameters and the width of parameter boundaries. This phenomenon is not due to a deficiency of the search method; rather, it arises because models with widely different parameter values can exhibit similar behavior [6,14].

4. Discussion

We have constructed an objective function that effectively compares the AP shape and firing statistics of a compartmental model against target data in simulated annealing-based parameter optimization. The recentering method of boundary management is a significant improvement over the wraparound method, regardless of the size of imposed physiologic boundaries. This is an important step forward in reproducing a range of neuronal responses whose dynamics depend on AP shape. Future studies will extend the objective function to include time-modulated firing rate error and will investigate the use of genetic algorithms based search [9].

Acknowledgments

This material is based upon work supported by the National Science Foundation under a grant (DBI-0305799) awarded in 2003, and by NIH grants DC05669 and RR16754.

References

[1] E. Av-Ron, P.-P. Vidal, Intrinsic membrane properties and dynamics of medial vestibular neurons: a simulation, Biol. Cybern. 80 (1999) 383–392.
[2] M.F. Cardoso, R.L. Salcedo, S.F. de Azevedo, The simplex-simulated annealing approach to continuous non-linear optimization, Comput. Chem. Eng. 20 (1996) 1065–1080.
[3] A.P. Davison, personal communication, 2004.
[4] A.P. Davison, J. Feng, D. Brown, A reduced compartmental model of the mitral cell for use in network models of the olfactory bulb, Brain Res. Bull. 51 (2000) 393–399.
[5] R. Fitzhugh, Impulses and physiological states in theoretical models of nerve membrane, Biophys. J. 1 (1961) 445–466.
[6] M.S. Goldman, J. Golowasch, E. Marder, L.F. Abbott, Global structure, robustness, and modulation of neuronal models, J. Neurosci. 21 (2001) 5229–5238.
[7] S.M. Highstein, A.L. Politoff, Relation of interspike baseline activity to the spontaneous discharges of primary afferents from the labyrinth of the toadfish, *Opsanus tau*, Brain Res. 150 (1978) 182–187.
[8] M.L. Hines, N.T. Carnevale, The NEURON simulation environment, Neural Comput. 9 (1997) 1179–1209.
[9] J.H. Holland, Adaptation in Natural and Artificial Systems, second ed., MIT Press, Cambridge, MA, 1992 ed. (University of Michigan Press, Ann Arbor, 1975).
[10] S.C. Kirkpatrick, D. Gelatt, M.P. Vechi, Optimization by simulated annealing, Science 220 (1983) 671–680.
[11] L.N. Marenco, C. Crasto, P.M. Nadkarni, P.L. Miller, G.M. Shepherd. NeuronDB, 2004, http://senselab.med.yale.edu/senselab/NeuronDB/
[12] J.S. Nagumo, S. Arimato, S. Yoshizawa, An active pulse transmission line simulating a nerve axon, Proc. IRE 50 (1962) 2061–2070.
[13] W.H. Press, S.A. Teukolsky, W.T. Vetterling, B.P. Flannery, Numerical Recipes in C: The Art of Scientific Computing, second ed., Cambridge University Press, Cambridge, UK, 1992.
[14] A.A. Prinz, D. Bucher, E. Marder, Similar network activity from disparate circuit parameters, Nat. Neurosci. 7 (2004) 1345–1352.
[15] P. Rothnie, J.C. Beck, H. Straka, R. Baker, S.L. Wearne. Contribution of velocity storage neural integrator neurons to VOR plasticity, in: Soc. Neurosci. Abstr., vol. 27, Program no. 405.2, 2001.
[16] G.Y. Shen, W.R. Chen, J. Midtgaard, G.M. Shepherd, M.L. Hines, Computational analysis of action potential initiation in mitral cell soma and dendrites based on dual patch recordings, J. Neurophysiol. 82 (1999) 3006–3020.

[17] W.R. Softky, C. Koch, The highly irregular firing of cortical cells is inconsistent with temporal integration of random EPSPs, J. Neurosci. 13 (1993) 334–350.
[18] M.C. Vanier, J.M. Bower, A comparative survey of automated parameter–search methods for compartmental neural models, J. Comput. Neurosci. 7 (1999) 149–171.

Christina Weaver is a postdoctoral fellow in the Department of Neuroscience at Mount Sinai School of Medicine (New York, NY). She received her B.S. (Hons) in mathematics from Mount St. Mary's College (1998), and her M.S. and Ph.D. in applied mathematics and statistics from Stony Brook University (2000 and 2003, respectively). She began her work at Mount Sinai as an NSF Postdoctoral Fellow in Interdisciplinary Informatics (2003–2005). Her research applies computational modeling techniques to investigate the contributions of morphology to neuronal firing dynamics, particularly in systems that exhibit neural integration and persistent activity.

Susan Wearne is a Mathematical Neuroscientist in the Center for Biomathematics and the Fishberg Department of Neuroscience, Mount Sinai School of Medicine, New York. She received her B.A. (Hons) in 1985 from the University of Sydney, Australia, with majors in mathematics and physiological psychology; her Ph.D. majoring in vestibular neuroscience from the University of Sydney in 1993, and her Masters in pure and applied mathematics from the University of New South Wales, Australia, in 1999. Her research interests include the physical and biological bases of fractional order dynamical systems, structural determinants of neural function, and biological bases of neural integration.